

Seeing phi meson through the dilepton spectra in heavy-ion collisions

W.S. Chung and C.M. Ko

*Cyclotron Institute and Department of Physics, Texas A&M University,
College Station, Texas 77843, U.S.A.*

G.Q. Li

*Department of Physics and Astronomy, State University of New York at Stony Brook,
Stony Brook, New York 11794, U.S.A.*

Dilepton spectra from the decay of phi mesons produced in heavy-ion collisions at SIS/GSI energies (~ 2 GeV/nucleon) are studied in the relativistic transport model. We include phi mesons produced from baryon-baryon, pion-baryon, and kaon-antikaon collisions. The cross sections for the first two processes are obtained from an one-boson-exchange model, while that for the last process is taken to be the Breit-Wigner form through the phi meson resonance. For dileptons with invariant mass near the phi meson peak, we also include contributions from neutron-proton bremsstrahlung, pion-pion annihilation, and the decay of rho and omega mesons produced in baryon-baryon and meson-baryon collisions. Effects due to medium modifications of the kaon and vector (rho, omega and phi) meson properties are investigated. We find that the kaon medium effects lead to a broadening of the dilepton spectrum as a result of the increase of phi meson decay width. Furthermore, the dropping of phi meson mass in nuclear medium leads to a shoulder structure in the dilepton spectrum besides the main peak at the bare phi meson mass. The experimental measurement of the dilepton spectra from heavy-ion collisions is expected to provide useful information about the phi meson properties in dense matter.

I. INTRODUCTION

The goal of relativistic heavy ion collisions is to study the properties of nuclear matter under extreme conditions, including extremely high density and/or temperature. This information is important for understanding the physics of the early universe and for studying the dynamic and static properties of stellar objects, like the structure of neutron stars and supernova explosion. It has been suggested that there may exist various phase transitions in the nuclear matter, such as the liquid-gas phase transition [1], the kaon condensation [2,3], the restoration of chiral symmetry [4], and the formation of the quark-gluon plasma [5]. These phase transitions, if they do occur in heavy ion collisions, will have significant phenomenological implications. For example, as a precursor to chiral symmetry restoration, hadron properties are expected to be modified in hot and dense matter [6], leading to significant effects on their production rate. To study the properties of hot and dense nuclear matter, heavy-ion accelerators have been constructed since mid-70s. At the relativistic energy regime, important facilities include the BEVALAC at Berkeley, the SIS at Darmstadt, the AGS at Brookhaven and the SPS at CERN. Still under construction are two ultra-relativistic colliders; the RHIC at BNL and the heavy ion program at CERN LHC.

To extract information about phase transitions and hadron in-medium properties from heavy ion experiments, different observables that are sensitive to the underlying theoretical parameters have been proposed. Among the important ones are the collective flow of various types [7] and particle production [8,9]. Dileptons, because of their relatively weak interaction with the dense environment, are particularly useful for studying the medium effects and phase transitions in heavy-ion collisions [10–13].

Dielectron production in the energy regime of 1-2 GeV/nucleon was studied by the DLS collaboration at the BEVALAC in Berkeley [14,15]. Because of the high hadron multiplicity the heaviest systems measured with DLS were reactions involving Ca+Ca. Also, the mass resolution of the DLS spectrometer is not sufficient to resolve the ω and ϕ peaks from the ρ distribution. A second generation detector HADES is currently under construction at GSI [16]. With its high counting rate capability and large geometrical acceptance, HADES is able to measure dielectron pairs for the heavy system U+U. With an invariant mass resolution better than 1%, a clear identification of the ω and ϕ peaks can be achieved.

At higher SPS energies, dilepton spectra have been measured by three collaborations: the CERES collaboration is specialized in the mass region up to about 1.5 GeV [17], the HELIOS-3 collaboration has measured dimuon spectra from its threshold up to the J/Ψ region [18], and the NA38/NA50 collaboration measures dimuon spectra in the intermediate- and high-mass region [19]. Recent observation of low-mass dilepton enhancement in heavy-ion collisions by the CERES and HELIOS-3 collaborations has led to the suggestions of various medium effects [20–22], including the dropping of vector meson masses in hot dense matter.

Theoretical studies on dilepton production at BEVALAC energies were carried out by Xiong *et. al.* [23] and Wolf *et. al.* [24]. They calculated the dilepton yield from proton-neutron (pn) bremsstrahlung, Δ Dalitz decay, $\pi\pi$ annihilation, pion annihilation on nucleon, and, in Ref. [24], also the η Dalitz decay. Their results indicate that the π^0 Dalitz decay dominates the invariant mass spectrum below the pion mass. The η Dalitz decay then dominates the spectrum up to an invariant mass of 450 MeV. Above 500 MeV, the most important channels are found to be pn bremsstrahlung and $\pi\pi$ annihilation. These studies reproduce well the original DLS data [14]. Recently published data from the DLS collaboration [15] show, however, a strong enhancement in the η mass region compared with the original data, implying that the η yield could be enhanced. This is, however, in conflict with the η yield and spectra measured by the TAPS collaboration for similar reactions [25].

In this paper, we will concern ourselves mainly with dilepton spectra from phi meson decay in heavy-ion collisions at energies available from the SIS at GSI, where experimental data will become available in the near future from the HADES collaboration. The study of phi meson in heavy ion collisions is interesting in view of the following considerations:

- First of all, phi meson is a pure $s\bar{s}$ state, and its production in hadronic interactions are therefore suppressed by the OZI rule [26]. This has led to the suggestion of identifying phi meson enhancement as a possible signature for the formation of the quark-gluon plasma in heavy-ion collisions [27].
- Phi meson decays chiefly into a kaon-antikaon pair. Since the mass of phi meson is very close to twice the kaon mass ($m_\phi - 2m_K = 0.032$ GeV), its width in free space is small (about 4.4 MeV). In nuclear medium, both kaon and phi meson masses may change. If the decrease of $m_K^* + m_{\bar{K}}^*$ is larger than that of m_ϕ^* , then the phi meson decay width would increase, leading to a broader phi meson mass spectrum. On the other hand, if the decrease of phi meson mass is larger than that of $m_K^* + m_{\bar{K}}^*$, its strong decay channel will be prohibited in the medium. The phi meson mass spectrum from heavy-ion collisions thus provides important information on the medium modification of both kaon and phi mesons. The suggestion of studying the kaon medium effects from phi meson production in heavy-ion collisions was first proposed by Shuryak and collaborators [28].

- In QCD sum-rule calculations [29], the change of phi meson mass is related to the nucleon strangeness content. Thus, the detection of in-medium phi meson mass is expected to provide indirect information about the nucleon strangeness content.
- Experimentally, phi meson can be detected from both its K^+K^- and dilepton decay channels. The main difference between these two channels is that in the K^+K^- case, the strong kaon and antikaon final-state interactions basically limit the detection of only those phi mesons that decay at and after freeze-out, while from the dilepton channel one can also detect phi mesons that decay inside the initial hot dense matter, i.e., before freeze-out. Therefore, a simultaneous measurement of the phi meson spectra in the K^+K^- and dilepton channels will provide useful information about the relative decay probabilities of phi mesons inside and outside the matter.

Phi meson production from heavy-ion collisions has already been studied at various energies. At SPS energies it was measured by the NA38 collaboration [30] and the HELIOS-3 collaboration [31] via the dimuon invariant mass spectra. A factor of 2 to 3 enhancement in the double ratio $(\phi/(\omega+\rho^0))_{SU(W)}/(\phi/(\omega+\rho^0))_{pW}$ was observed. Various theoretical attempts have been made to understand this enhancement [32–34]. In particular, an enhancement of the phi meson yield may be a signature of the formation of a quark-gluon plasma in the collisions [27]. However, the enhancement can also be explained in hadronic models if one takes into account the reduced phi meson mass in medium [32] or the formation of color ropes in the initial stage of the collisions [33].

The phi meson yield has also been measured at AGS/BNL by the E802 collaboration in central collisions between a 14.6 AGeV/c Si beam and a Au target [35]. They are identified from the invariant mass spectrum of K^+K^- pairs, and the measured phi meson mass and width are found to be consistent with those in free space. The ratio of the phi meson yield to the K^- yield is about 10%, which can be understood if thermal and chemical equilibrium with a temperature of about 110 MeV are assumed at freeze out [36,37]. On the other hand, calculations based on the coalescence model [38], in which the phi meson is formed from the kaon and antikaon at freeze out, underestimate the data by a large factor, indicating that processes other than kaon-antikaon annihilation should dominate phi meson production at these energies.

Phi meson production from heavy-ion collisions at SIS/GSI energies is being studied by the FOPI collaboration [39] through the K^+K^- invariant mass distribution. A total of $30 \pm 8 \phi$ has been reconstructed in the reaction Ni+Ni at 1.93 GeV/nucleon from an event sample of 7×10^6 events. Based on these preliminary results it has been concluded that the phi meson yield is about 10% of the K^- yield, which is very similar to that observed at the AGS energies. This is somewhat surprising since the SIS energies are below the phi meson production threshold in the nucleon-nucleon collision in free space, while the AGS energies are well above the threshold. In Ref. [40], we have studied phi meson production from heavy-ion collisions at these energies through its KK decay channel. Comparison of the phi meson yield from the transport model with the preliminary data from the FOPI collaboration [39] seems to indicate that medium effects on phi meson play a non-negligible role. The present work is a continuation of Ref. [40]. Our main motivation is to examine the feasibility of detecting directly the reduction of phi meson mass in nuclear medium from the dilepton invariant mass spectrum from heavy ion collisions, which will be measured by HADES in the near future [16].

Theoretical studies of the dilepton decay of phi mesons in heavy ion collisions at SIS energies have been carried out in Ref. [13] by assuming that they are only produced from KK annihilation. It was found that for dileptons with invariant mass around m_ϕ , contributions from $\pi\pi$ annihilation and phi meson decay are comparable. As shown in Ref. [40], ϕ mesons can also be produced from baryon-baryon collisions and pion-baryon collisions. Because of the larger abundance of pions and nucleons than kaons, these two channels were found to be more important than the KK channel. One thus expect that including these contributions in the transport model would raise the ϕ peak in the dilepton mass spectrum to above the background from $\pi\pi$ annihilation and also other background studied in Refs. [23,24]. In addition, we will also consider the background from direct leptonic decay of rho and omega mesons produced from baryon-baryon and pion-baryon interactions.

This paper is arranged as follows. In Section 2 we review the theoretical predictions for the properties of vector mesons and kaon meson in dense matter. In Section 3 we discuss the elementary cross sections for vector meson and kaon production in baryon-baryon and meson-baryon interactions. The results and discussions of dilepton production from heavy ion collisions are then presented in Section 4. The paper ends with a brief conclusion in Section 5.

II. IN-MEDIUM PROPERTIES OF MESONS

In this section, we review briefly various theoretical predictions for the in-medium properties of vector mesons and kaons. Details can be found in a recent review by two of the authors [41].

A. vector mesons

Various approaches and models have been used to study theoretically the vector meson masses in nuclear matter. These include the scaling anatz of Brown and Rho [6], the QCD sum-rule approach [29,42–45], the quark-meson coupling model [46], and the quantum hadrodynamics (QHD) [47–49]. All these studies seem to suggest that decreasing vector meson masses is a generic consequence of chiral symmetry restoration at high densities and/or temperature.

Studies on vector meson in-medium masses using the QCD sum rules were first carried out by Hatsuda and Lee [29]. In this approach, the real part of the current-current correlation function is expressed in terms of the scalar quark and gluon condensates after using the operator product expansion(OPE) at short distances. The imaginary part is, on the other hand, parameterized phenomenologically. Using the dispersion relation to relate the real and imaginary parts, vector meson masses are found to satisfy certain sum rules involving the quark and gluon condensates. To extend this approach to vector mesons in nuclear medium, one needs to include not only the density dependence of the condensates but also non-scalar condensates. With a simple delta-function plus continuum for the rho meson spectral function, Hatsuda and Lee obtained the following results for the in-medium vector meson masses [29]

$$\frac{m_{\rho,\omega}^*}{m_{\rho,\omega}} \approx 1 - (0.16 \pm 0.06) \frac{\rho}{\rho_0} \quad (1)$$

$$\frac{m_\phi^*}{m_\phi} \approx 1 - (0.15 \pm 0.05) y \frac{\rho}{\rho_0}. \quad (2)$$

The uncertainties in the above expressions are due to uncertainties in the density dependence of the condensates. At normal nuclear matter density, ρ_0 , rho and omega meson masses thus drop by about 20%. For phi meson, the in-medium mass depends on the nucleon strangeness content y . Taking $y = 0.15$, the phi meson mass is seen to drop by about 2% at normal nuclear matter density.

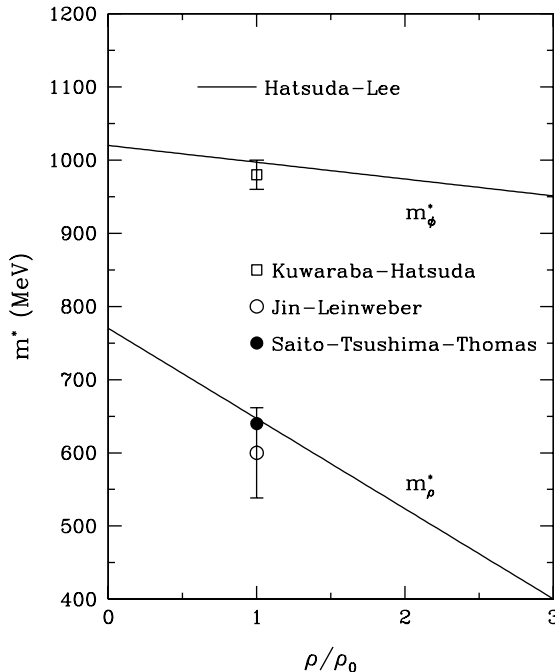


FIG. 1. Vector meson masses as functions of density as obtained in different theoretical approaches.

The QCD sum rules for vector mesons were reanalyzed in Ref. [42] by assessing the uncertainties of the condensates and other inputs using the Monte Carlo error analysis. It was found that at normal nuclear matter density $m_\rho^*/m_\rho \approx 0.78 \pm 0.08$, in agreement with the findings of Ref. [29].

The assumption that the rho meson spectral function in nuclear medium is the sum of a delta function and a continuum is, however, too simplistic, as the rho meson has a large decay width in free space and it also interacts strongly with nucleons. An improved QCD sum-rule calculation was carried out by Asakawa and Ko [43] using a more realistic rho meson spectral function. They found a similar decrease of the rho meson mass with density as that of Ref. [29]. More recently, another realistic study of rho meson spectral function has been carried out in Ref. [44], and it is found the rho meson mass does not change but its width becomes larger. This rho spectral function also satisfies the QCD sum rules. According to Lipold *et al.* [45], the QCD sum rules do not give a stringent constraint on the rho meson spectral function as they can be satisfied either with a reduced mass and width or a larger width but without much change in its mass.

The quark-meson coupling model has also been used to study the density dependence of hadron masses [46]. In this model, the vector meson is treated as an MIT bag with two light quarks which are coupled to the vector and scalar fields generated by the nuclear medium. It was found that at normal nuclear matter density the rho and omega meson masses drop by about 17%, in agreement with the QCD sum-rule predictions.

Various hadronic models have also been used to study the medium effect on vector meson masses. Calculations that only include the polarization of the Fermi sea predict that ω and ρ meson masses either increase or stay more or less the same in nuclear matter [50,51]. The effect of vacuum polarization or the polarization due to nucleons in the Dirac sea was studied in Refs. [47–49] and found to dominate over the Fermi sea polarization, leading thus to decreasing rho and omega meson masses. For phi meson, both nucleon and hyperon vacuum polarization contribute, leading to a reduction of its mass by about 2-3% at normal nuclear matter density as in QCD sum-rule studies [52]. In the vector dominance model, inclusion of dropping kaon-antikaon in-medium mass also leads to a decrease of phi meson mass in nuclear medium [53,54].

The results from Refs. [29,42,46,52] for vector meson in-medium masses are summarized in Fig. 1. In this work, as in Refs. [13,40], we use the results of Hatsuda and Lee [29] for the density dependence of vector meson masses and linearly extrapolate it to high densities.

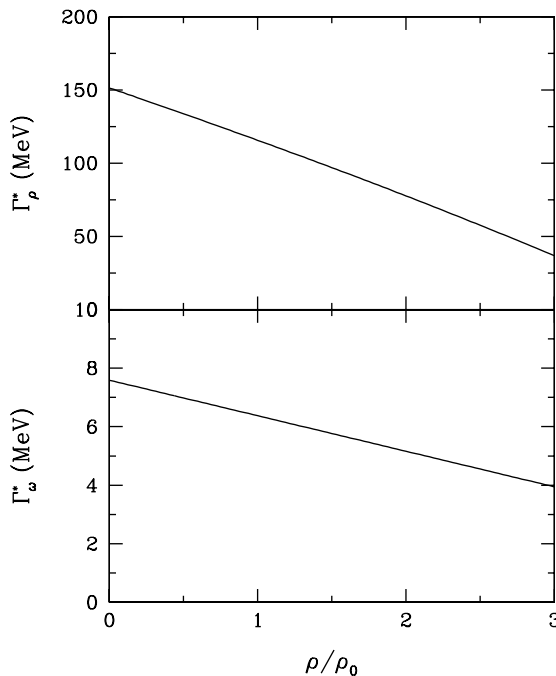


FIG. 2. Rho and omega meson decay widths as a function of density.

Because of the change in vector meson masses, their decay widths are also modified. The rho meson decays dominantly to two pions with the following decay width in nuclear matter,

$$\Gamma_\rho^* = \frac{g_{\rho\pi\pi}^2}{4\pi} \frac{1}{12m_\rho^{*2}} (m_\rho^{*2} - 4m_\pi^2)^{3/2}, \quad (3)$$

where the coupling $g_{\rho\pi\pi}^2/4\pi \approx 2.9$ is determined from its decay width in free space.

The omega meson decays mostly to three pions. Without a hadronic model the functional form of the decay width cannot be given. Here we simply assume that its decay width is proportional to its in-medium mass, i.e.,

$$\Gamma_\omega^* \approx \Gamma_\omega \frac{m_\omega^*}{m_\omega}. \quad (4)$$

The density dependence of the rho and omega meson decay widths is shown in Fig. 2.

B. kaons

Since phi mesons decay predominantly into $K\bar{K}$ pairs, it is necessary to address the issue of kaon medium effects. It has been proposed [28] that the phi meson yield can also be used as a signature for the medium effect on kaons. A reduced kaon in-medium mass increases $\Gamma_{\phi \rightarrow K\bar{K}}$, so phi mesons are more likely to decay before freeze out, leading to a lower yield of final phi mesons that can be detected through their decay into K^+K^- pairs. A cleaner signature can be observed from the width of the phi meson peak in the dilepton invariant mass spectrum. A significantly broadened peak can be another signature of the kaon medium effect.

Since the pioneering work of Kaplan and Nelson [2] on the possibility of kaon condensation in nuclear matter, a large amount of theoretical efforts have been devoted to the study of kaon properties in dense matter, using such diversified approaches as the chiral Lagrangian [55–60], the Nambu–Jona-Lasinio model [61], and the SU(3) Waleckatype mean-field model [62,63]. Although quantitative results from these models are not identical, a consistent picture has emerged qualitatively; namely, in nuclear matter the K^+ feels a weak repulsive potential, whereas the K^- feels a strong attractive potential. Most experimental data for strangeness production and collective flow in heavy ion collisions at SIS energies [64] have been found to support the existence of these medium effects [65–68]. The kaon and antikaon potentials also have observable effects on kaon azimuthal distributions [69] and antikaon flow [70].

We will consider two scenarios for kaon properties in nuclear medium, one with and one without medium modification. From the chiral Lagrangian the kaon and antikaon in-medium masses can be written as [66]

$$m_K^* = [m_K^2 - a_K \rho_S + (b_K \rho)^2]^{1/2} + b_K \rho, \quad (5)$$

$$m_{\bar{K}}^* = [m_{\bar{K}}^2 - a_{\bar{K}} \rho_S + (b_K \rho)^2]^{1/2} - b_K \rho, \quad (6)$$

where $b_K = 3/(8f_\pi^2) \approx 0.333 \text{ GeV}\cdot\text{fm}^3$, a_K and $a_{\bar{K}}$ are two parameters that determine the strength of the attractive scalar potential for kaon and antikaon, respectively. If one considers only the Kaplan-Nelson term, then $a_K = a_{\bar{K}} = \Sigma_{KN}/f_\pi^2$. In the same order, there is also a range term which acts differently on kaon and antikaon, and leads to different scalar attractions. Since the exact value of Σ_{KN} and the size of the higher-order corrections are still under debate, we take the point of view that $a_{K,\bar{K}}$ can be treated as free parameters and try to constrain them from the experimental observables in heavy-ion collisions. In Ref. [66] it was found that $a_K \approx 0.22 \text{ GeV}^2\cdot\text{fm}^3$ and $a_{\bar{K}} \approx 0.45 \text{ GeV}^2\text{fm}^3$ provide a good description of the kaon and antikaon spectra from Ni+Ni collisions at 1 and 1.8 AGeV. These values will be used in this work as well. The density dependence of the kaon and antikaon masses is shown in Fig. 3.

Because of the change of phi and/or kaon masses with nuclear density, the phi meson decay width is also modified. According to Ref. [13], the phi meson decay width is given by

$$\Gamma_\phi^* = \frac{g_{\phi K\bar{K}}}{4\pi} \frac{1}{6m_\phi^{*5}} [(m_\phi^{*2} - (m_K^* + m_{\bar{K}}^*)^2)(m_\phi^{*2} - (m_K^* - m_{\bar{K}}^*)^2)]^{3/2}. \quad (7)$$

In Fig. 4, we show the density dependence of the phi meson decay width in three different scenarios for phi and kaon masses. Generally, the phi meson decay width is seen to increase with density if kaon medium effects or both kaon and phi medium effects are included. In the latter case, the dropping of $m_K^* + m_{\bar{K}}^*$ is apparently more significant than that of m_ϕ^* .

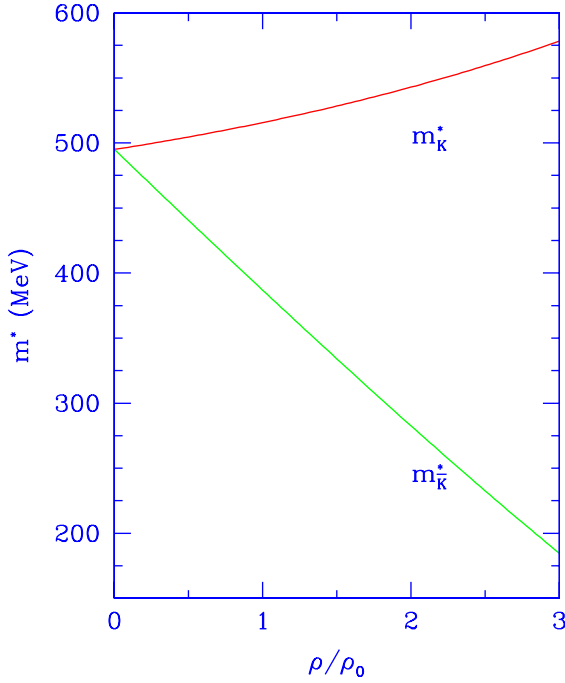


FIG. 3. Kaon and antikaon masses as functions of density as determined in Ref. [66].

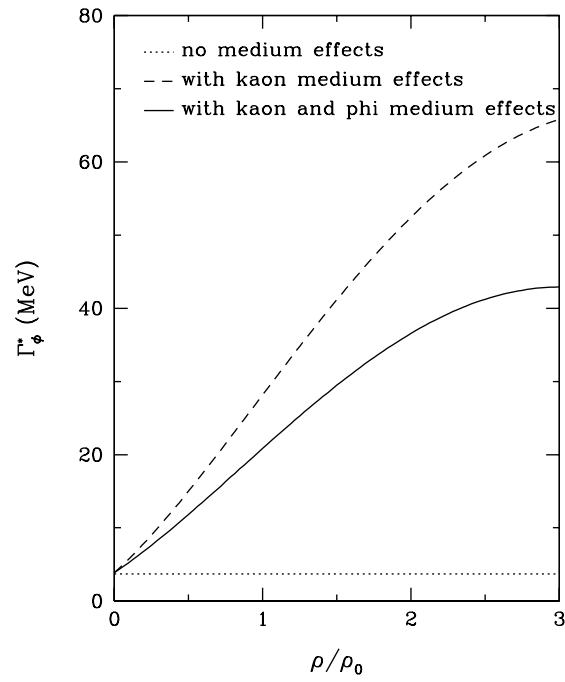


FIG. 4. Phi meson decay widths in three scenarios: without medium effects (dotted curve), with kaon medium effects (dashed curve), and with both kaon and phi medium effects (solid curve).

III. PARTICLE PRODUCTION CROSS SECTIONS

One of the most important inputs in the transport model for particle production from heavy-ion collisions is the elementary particle production cross section in hadron-hadron interactions. In this section we shall discuss the vector meson and kaon production cross sections that are used in the present work. We will also discuss dilepton production cross sections from pn bremsstrahlung and pion-pion annihilation, as well as the decay widths of vector mesons into dileptons.

A. phi meson production

In heavy-ion collisions at SIS energies, the most abundant particles are nucleons, Δ resonances, and pions. Phi meson can thus be produced from reactions such as $NN \rightarrow NN\phi$, $N\Delta \rightarrow NN\phi$, $\Delta\Delta \rightarrow NN\phi$, $\pi N \rightarrow \phi N$, and $\pi\Delta \rightarrow \phi N$. In addition, phi meson can also be formed from kaon-antikaon annihilation, which has a cross section of usual Breit-Wigner form

$$\sigma(K\bar{K} \rightarrow \phi) = \frac{3\pi}{k^2} \frac{(m_\phi\Gamma_\phi)^2}{(M^2 - m_\phi^2)^2 + (m_\phi\Gamma_\phi)^2}, \quad (8)$$

where M is the invariant mass of the kaon-antikaon pair and k is the magnitude of the kaon momentum in the center-of-mass frame.

The cross sections for the other processes listed above have been studied in Ref. [40] based on an one-boson exchange model. For the reaction $\pi B \rightarrow \phi N$, where B denotes either a nucleon or a Δ resonance, rho meson exchange is used, while both rho and pion exchange are introduced for the reaction $BB \rightarrow NN\phi$. Coupling constants needed for evaluating these cross sections are either taken from the Bonn model for NN potential [71] or determined from the measured width for $\phi \rightarrow \pi\rho$. Most cut-off parameters at the interaction vertices are also taken from the Bonn model. Since the exchanged rho and pion are virtual, two cut-off parameters at the $\phi\pi\rho$ vertex are introduced, and they are determined by fitting to available experimental data for the reactions $\pi^-p \rightarrow \phi n$ and $pp \rightarrow pp\phi$ [72]. This model is then extended, without introducing further adjustable parameters, to calculate the cross sections involving baryon resonances.

B. rho and omega meson production

An important background for the dilepton spectrum around phi meson mass comes from the tail part of the dilepton spectra from the decay of omega and rho mesons, which are produced from baryon-baryon and pion-baryon interactions. The rho meson can also be formed in pion-pion annihilation. In this work, we treated the dilepton spectrum from pion-pion annihilation using the so-called form factor approaches [13], i.e., without considering the explicit formation and propagation of rho meson from pion-pion annihilation.

Several parameterizations have been proposed for the rho and omega meson production cross sections in pion-nucleon interactions [73–75]. These parameterizations have been used in studying vector meson production in pion-nucleus [76] and proton-nucleus [77] reactions through their dilepton decays. Here we shall follow the one introduced in Ref. [74]. For rho meson production, experimental data for the four channels, $\pi^+p \rightarrow \rho^+p$, $\pi^+n \rightarrow \rho^0p$, $\pi^-p \rightarrow \rho^-p$, and $\pi^-p \rightarrow \rho^0n$ [72], show that their cross sections are similar and can be parameterized by

$$\begin{aligned} \sigma(\pi^-p \rightarrow \rho^0n) &= 9.75(\sqrt{s} - \sqrt{s_0})^{0.844} \text{ mb}, \quad \sqrt{s} \leq 2 \text{ GeV} \\ &= 64.1s^{-2.11} \text{ mb}, \quad \sqrt{s} > 2 \text{ GeV}, \end{aligned} \quad (9)$$

where $\sqrt{s_0} = m_N + m_\rho$ is the threshold. This parameterization is slightly different from that proposed in Ref. [74], in order to better fit the data for $\pi^-p \rightarrow \rho^0n$ near the threshold. Comparison of this parameterization with the experimental data is shown in Fig. 5.

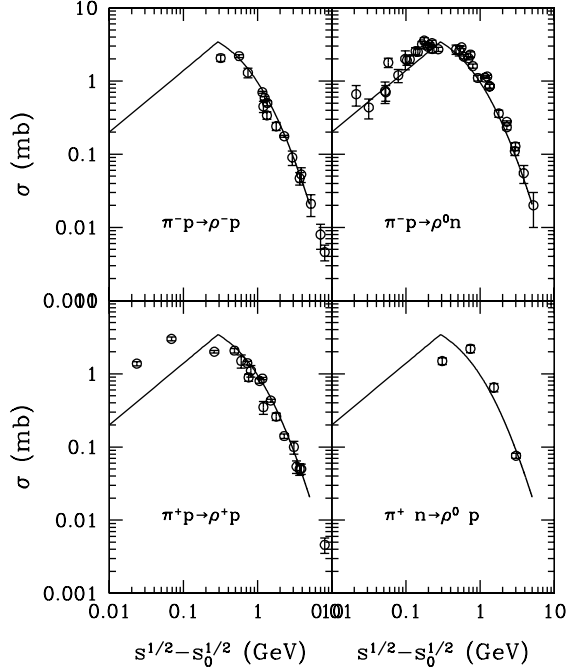


FIG. 5. Comparison of the theoretical parameterization, Eq. (9), with the experimental data for $\pi N \rightarrow \rho N$.

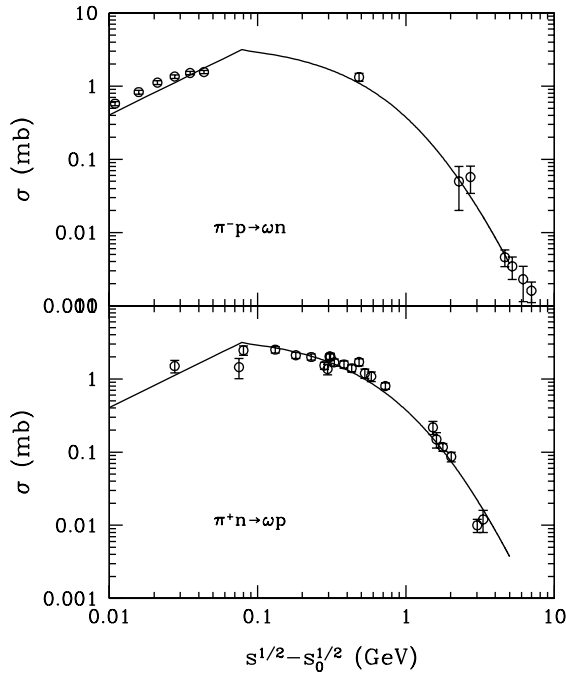


FIG. 6. Comparison of the theoretical parameterization, Eq. (10), with the experimental data for $\pi N \rightarrow \omega N$.

Similarly, available experimental data for omega meson production in pion-nucleon collisions can be fitted by the following parameterization, which is taken from Ref. [74],

$$\begin{aligned}\sigma(\pi^- p \rightarrow \omega n) &= 40.43(\sqrt{s} - \sqrt{s_0}) \text{ mb}, \quad \sqrt{s} \leq 1.8 \text{ GeV} \\ &= 61.57s^{-2.55} \text{ mb}, \quad \sqrt{s} > 1.8 \text{ GeV},\end{aligned}\quad (10)$$

where $\sqrt{s_0} = m_N + m_\omega$ is the threshold. Comparison of this parameterization with the experimental data is shown in Fig. 6.

Rho and omega production from the nucleon-nucleon interaction has been studied in Ref. [74] using an one-boson-exchange model, assuming that these processes can be factorized into a two step process. A form factor is introduced to account for the virtuality of the pion. Furthermore, simple parameterizations were proposed. Here we use a somewhat different form of parameterization, which has been used also for the parameterization of the eta meson production cross section in proton-proton collision near the threshold [24], i.e.,

$$\sigma(pp \rightarrow pp\rho^0) = \frac{0.393(\sqrt{s} - \sqrt{s_0})}{1.05 + (\sqrt{s} - \sqrt{s_0})^2} \text{ mb}, \quad (11)$$

where $\sqrt{s_0} = 2m_N + m_\rho$ is the threshold, and

$$\sigma(pp \rightarrow pp\omega) = \frac{0.219(\sqrt{s} - \sqrt{s_0})}{1.238 + (\sqrt{s} - \sqrt{s_0})^2} \text{ mb}, \quad (12)$$

with the threshold $\sqrt{s_0} = 2m_N + m_\omega$. Comparison of these parameterizations with experimental data and the parameterizations from Ref. [74] are shown in Figs. 7 and 8.

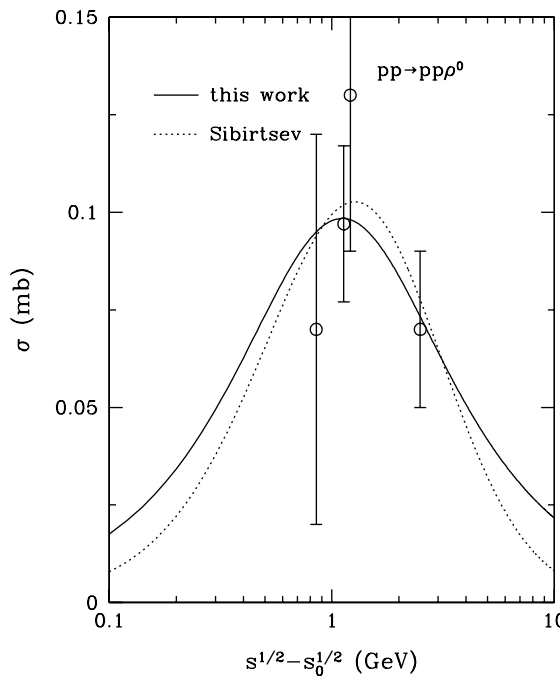


FIG. 7. Comparison of the theoretical parameterizations with the experimental data for $pp \rightarrow pp\rho^0$. The solid line is from this work, and the dotted line is from Ref. [74].

The cross sections for rho and omega production from other isospin channels of nucleon-nucleon interactions are not available in Ref. [74]. Here we simply assume that are the same as those for proton-proton interactions. Vector mesons can also be produced in these processes with nucleons replaced by Δ 's. These cross sections cannot be studied experimentally. Here we follow the usual procedure used in transport models by assuming that these cross sections are the same as those for the corresponding nucleon channels.

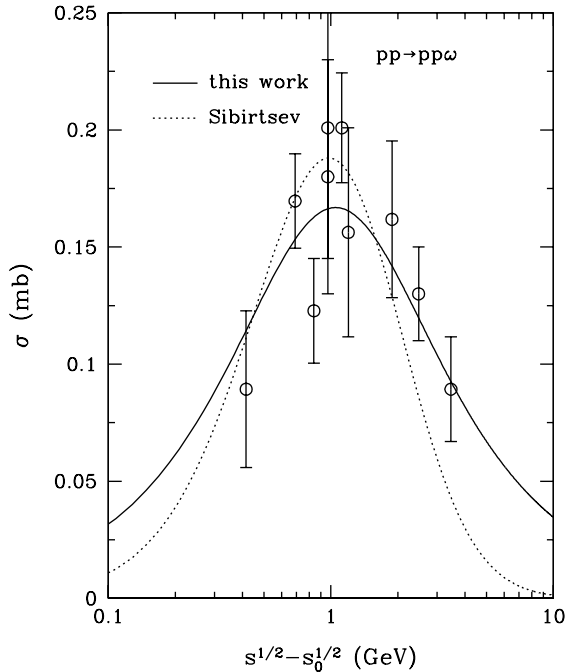


FIG. 8. Same as Fig. 7 for $pp \rightarrow pp\omega$.

C. kaon and antikaon production

In heavy-ion collisions at incident energies considered in this work, kaons can be produced from pion-baryon and baryon-baryon collisions. For the former we use the cross sections obtained in the resonance model by Tsushima *et al.* [78]. For the latter the cross sections obtained in the one-boson-exchange model of Ref. [79] are used. Both models describe the available experimental data very well. For antikaon production from pion-baryon collisions we use the parameterization proposed by Sibirtsev *et al.* [80]. For baryon-baryon collisions, we use a somewhat different parameterization, which describes the experimental data better than Ref. [80]. In addition, the antikaon can also be produced from strangeness-exchange processes such as $\pi Y \rightarrow \bar{K}N$, where Y is either a Λ or Σ hyperon [81]. Cross sections for these processes are obtained from the inverse ones, $\bar{K}N \rightarrow \pi Y$, by the detailed-balance relation. All parameterizations for the elementary cross sections and comparisons with experimental data can be found in Ref. [66].

D. final-state interactions

Particles produced in elementary hadron-hadron interactions in heavy-ion collisions cannot escape the hadronic matter freely. Instead, they are subjected to strong final-state interactions. For kaons, because of strangeness conservation, their scattering with nucleons at low energies is dominated by elastic and pion production processes, which do not affect its final yield but change its momentum spectrum. The final-state interaction for the antikaon is much stronger. Antikaons can be destroyed in the strangeness-exchange processes, and they also undergo elastic scattering. Both the elastic and absorption cross sections increase rapidly with decreasing antikaon momenta.

Final-state interactions for phi meson were analyzed in Ref. [40]. These include both absorption and elastic rescattering by nucleons. Of all absorption processes considered, the $\phi N \rightarrow \Lambda K$, which is not OZI suppressed, was found to be the most important. In this work we follow Ref. [40] for the treatment of phi meson final-state interactions.

We also consider the absorption and rescattering of rho and omega mesons. Reactions such as $\omega N \rightarrow \pi N$, $\pi\Delta$ and $\rho N \rightarrow \pi N$, $\pi\Delta$ are included. Cross sections for these reactions can be found from those of the reversed processes

and the detailed balance relations. The cross sections for ωN and ρN elastic scattering have been extracted from the cross sections of the corresponding photoproduction processes using the photo-dissociation model [82]. It is found to be 5.6 mb at p_{lab} around 3 GeV. As elastic scattering does not change the dilepton yield, its effect on the dilepton spectrum is not expected to be significantly. We thus assume that their cross sections take a constant value in the energy range relevant for our calculations.

E. dilepton production

A vector meson can decay directly into a lepton pair. We use the following mass-dependent leptonic decay width for vector mesons [20],

$$\Gamma_{V \rightarrow e^+ e^-}(M) = C_{e^+ e^-} \frac{m_V^4}{M^3}, \quad (13)$$

where M is the mass of the vector meson, while m_V is its mass at the centroid. From the measured widths, the coefficient $C_{e^+ e^-}$ is determined to be 8.814×10^{-6} , 0.767×10^{-6} , and 1.334×10^{-6} for ρ^0 , ω , and ϕ decay, respectively. To obtain the final dilepton spectra from vector meson decays, we need to integrate over time and add also the contribution after the freeze-out. Denoting $dP_\phi(t)/dt$ the differential probability of finding phi mesons at time t , the dilepton invariant mass spectrum from phi meson decays is then given by

$$\frac{dP_{e^+ e^-}}{dM} = \int_0^{t_f} \frac{dP_\phi(t)}{dM} \Gamma_{\phi \rightarrow e^+ e^-}(M) dt + \frac{dP_\phi(t_f)}{dM} \frac{\Gamma_{\phi \rightarrow e^+ e^-}(M)}{\Gamma_\phi(M)}. \quad (14)$$

The freeze-out time t_f follows automatically in the transport model when particle collisions become negligible. The first term in the above expression gives the contribution from phi meson decay ‘inside’ the fire ball, and the second term gives that from decay ‘outside’ the fire ball. Similar procedures are used for dileptons from rho and omega meson decays.

In addition, we shall also include dileptons from pn bremsstrahlung and pion-pion annihilation. Our procedure for pn bremsstrahlung is the same as in Xiong *et. al.* [23]. In the soft-photon approximation and including the phase-space correction, the differential cross section for dileptons with invariant mass M is given by:

$$\frac{d\sigma}{d^3 \mathbf{p} dM} \simeq \frac{\alpha^2}{6\pi^3} \frac{\bar{\sigma}(s)}{ME^3} \frac{R_2(\sqrt{s_2})}{R_2(\sqrt{s})} \quad (15)$$

where

$$R_2(s) = \sqrt{1 - \frac{4m^2}{s}},$$

$$s_2 = s + M^2 - 2E\sqrt{s},$$

$$\bar{\sigma}(s) = \frac{s - 4m^2}{2m^2} \sigma(s).$$

In the above, α is the fine structure constant, E and \mathbf{p} are the total energy and momentum of the dilepton pair, respectively, $\sigma(s)$ is the cross section of nucleon-nucleon elastic scattering, while m is the nucleon mass.

The dilepton production cross section from pion-pion annihilation is well-known [12,13], i.e.,

$$\sigma(M) = \frac{4\pi\alpha^2}{3M^2} \sqrt{1 - \frac{4m_\pi^2}{M^2}} |F_\pi|^2, \quad (16)$$

where the pion electromagnetic form factor is given by:

$$|F_\pi|^2 = \frac{m_\rho^4}{(M^2 - m_\rho^2)^2 + m_\rho^2 \Gamma_\rho^2}, \quad (17)$$

in terms of the rho meson mass m_ρ and width Γ_ρ .

IV. RESULTS AND DISCUSSIONS

As in Ref. [40], the dynamical evolution of heavy-ion collisions at SIS energies is described by the relativistic transport model, originally developed in Ref. [83] and extensively used in studying medium effects in heavy ion collisions [9]. As we are mainly interested in the possibility of seeing phi and kaon medium effects on the dilepton spectra, we shall present our results in the mass region from 0.8 to 1.2 GeV in central Ni+Ni collisions at 1.93 AGeV.

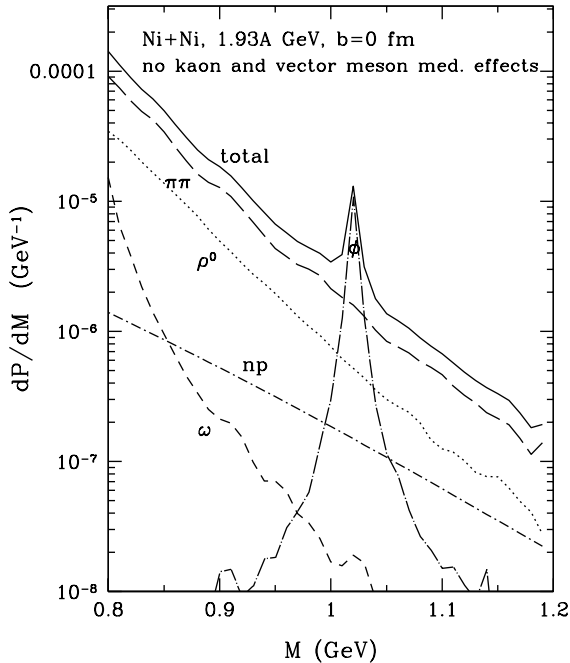


FIG. 9. Dilepton invariant mass spectra in central Ni+Ni collisions at 1.93A GeV. The results are for the scenario neglecting both the kaon and vector meson medium effects.

In Fig. 9 we show the dilepton invariant mass spectra in the case that both vector and kaon medium effects are neglected. Here, as well as in the following figures, the histogram bin size is taken to be 10 MeV, corresponding roughly to the mass resolution of HADES in the phi meson mass region. The major background around phi meson peak comes from $\pi\pi$ annihilation. The contribution from direct rho meson decay is about a factor of 3 below that from $\pi\pi$ annihilation. Furthermore, the contribution from pn bremsstrahlung is about one order of magnitude smaller than other background in this mass region. Finally, the contribution from direct omega meson decay is insignificant due to its narrow mass distribution. A well defined phi meson peak is seen in the dilepton spectrum, reflecting its small decay width of about 4 MeV. Overall the phi meson peak is about a factor 4-5 above the background. This make its detection relatively easy if the mass resolution is about 1%.

In the second scenario, we turn on the kaon medium effects as were required to explain the measured kaon yields and flow [64–68]. As shown in Fig. 4, because of the opening-up of the phase space, the phi meson decay width increases substantially in nuclear medium. As a result, phi mesons tend to decay faster and therefore less number of phi mesons can be detected via the K^+K^- channel. In Ref. [40] we found that the inclusion of kaon medium effects reduces the phi meson yield determined from the K^+K^- analysis by about a factor of two. Furthermore, the increase of phi meson decay width broadens its mass distribution and results in a large apparent width in the dilepton spectrum. The results in this scenario are shown in Fig. 10. As medium effects on vector mesons are neglected, the background is the same as in Fig. 9. Because of the increase of phi meson decay width, the dilepton mass spectrum from phi mesons becomes much broader than in Fig. 9, with a width of about 30-40 MeV. Consequently, the height of the peak is substantially reduced, and the phi meson peak is now below the background from $\pi\pi$ annihilation, leading to a broad bump instead of a sharp peak around m_ϕ in the total dilepton spectrum.

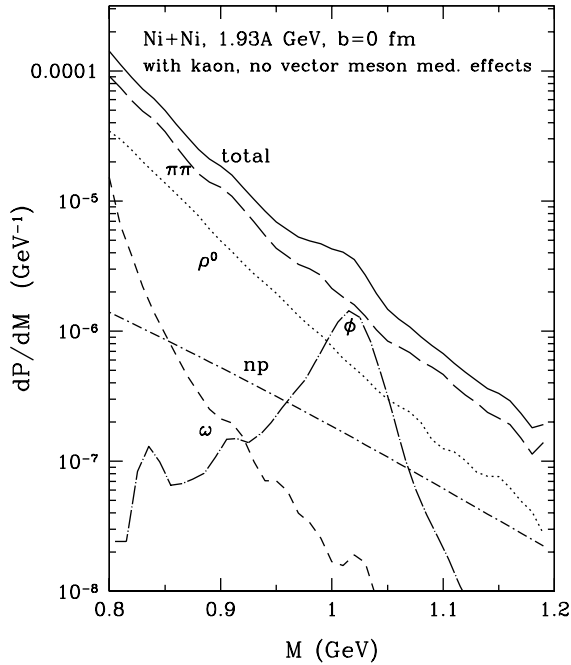


FIG. 10. Same as Fig. 9 for the scenario including kaon medium effects but neglecting vector meson medium effects.

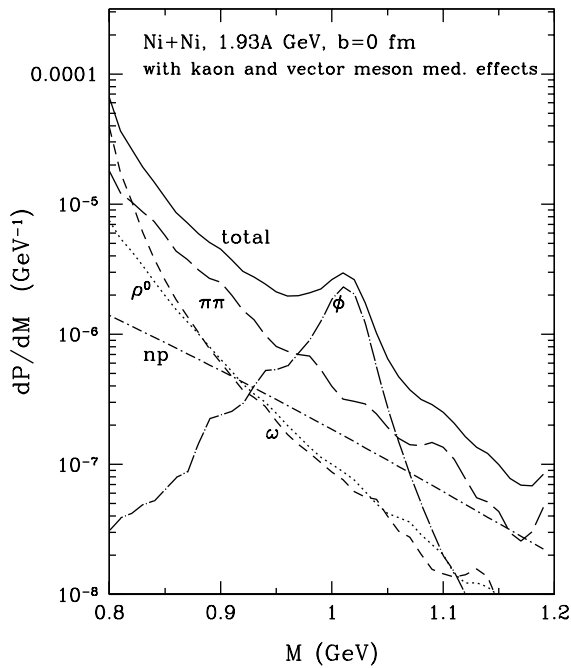


FIG. 11. Same as Fig. 9 for the scenario including both kaon and vector meson medium effects.

The results in the case with both kaon and vector meson medium effects are shown in Fig. 11. The most important background around the phi meson is still from $\pi\pi$ annihilation, which is, however, significantly smaller than in the case without vector meson medium effects. This is mainly due to the dropping rho meson mass that shifts the strength to masses below m_ρ . Although the rho meson yield is enhanced due to its dropping mass, they contribute mainly to dileptons with masses below m_ρ . On the other hand, the contribution from direct omega meson decay is enhanced in the dropping mass scenario, and it becomes comparable to that from direct rho meson decay. This is due to the enhanced production of omega meson, and the fact that most omega mesons decay after the freeze-out, when their masses return to the free ones. In this case the ϕ peak is about a factor of 3-4 above the background. Furthermore, there appears a shoulder around the invariant mass of 0.95 GeV, arising from the decay of phi mesons inside the fireball. Unfortunately, the height of the shoulder is about a factor of 2 below the background. In the total dilepton spectrum, an outstanding and broad peak instead of a weak bump is seen.

In Fig. 12 we summarize the dilepton spectra from phi meson decay in the three scenarios discussed above. In the scenario without medium effects, a very sharp phi peak is seen with a width of about 4 MeV. Including kaon medium effects that increases the phi meson decay width, the dilepton spectrum from phi meson decay becomes much broader with a width of about 30-40 MeV, and its height is substantially reduced. In the scenario with both decreasing kaon and vector meson in-medium masses, the dilepton spectrum is also quite broad with a width of about 30-40 MeV. Its height increases, however, by about a factor of 2 with respect to the second scenario, reflecting the fact that the phi meson yield is increased due to a reduced mass. A shoulder, although not very prominent, also develops around 0.95 GeV as a result of the decay of phi mesons inside the fireball.

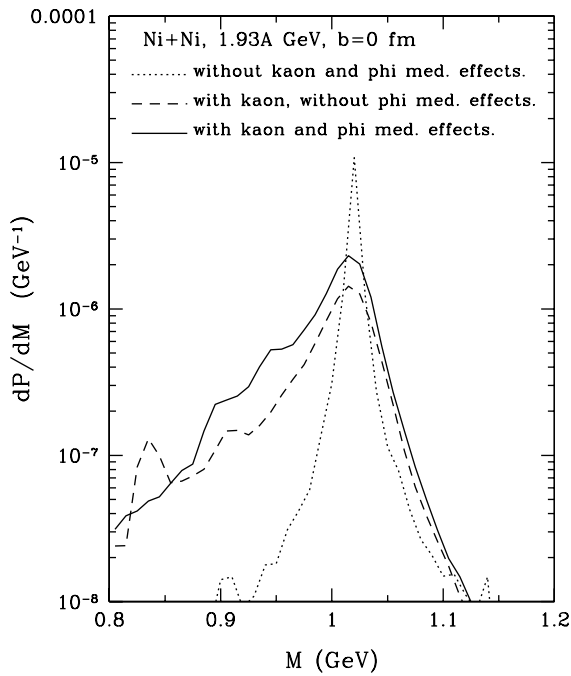


FIG. 12. Dilepton invariant mass spectra from phi meson decays in central Ni+Ni collisions at 1.93A GeV.

Our studies thus show that it will be quite difficult to isolate or extract from the measured dilepton spectrum the contribution from phi mesons. It is therefore useful to identify the characteristic differences in the total dilepton spectra from the three scenarios. This is shown in Fig. 13. The dotted curves in the figure show the background in the three scenarios, with those of the first and second scenario being the same. With the HADES mass resolution of about 1%, we expect to see a sharp peak in the dilepton spectrum which is about a factor of 5 above the background, if there are no medium effects on both kaon and vector mesons. On the other hand, a weak bump around m_ϕ would indicate that the phi meson mass distribution becomes broader as a result of kaon medium effects. Finally, if a broad and significant peak is seen around m_ϕ together with a shoulder around 0.95 GeV, this could be a good indication for the existence of both kaon and vector meson medium effects.

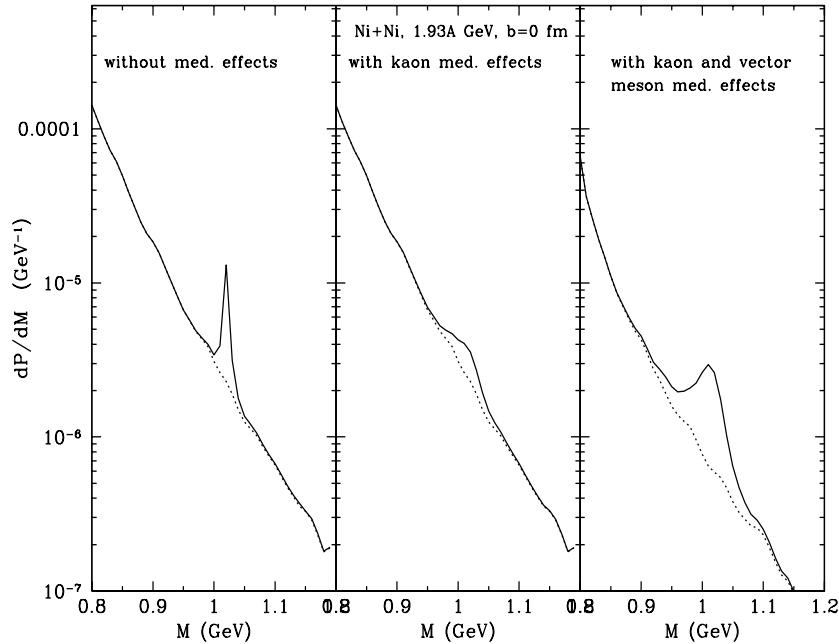


FIG. 13. Dilepton invariant mass spectra in central Ni+Ni collisions at 1.93A GeV. The dotted curves give the total background.

V. CONCLUSION

In conclusion, continuing our previous investigation on phi meson production from heavy-ion collisions [40], we studied in this paper the possibility of seeing the phi meson through its dilepton spectrum. To make a quantitative prediction, we have included contributions to dileptons with invariant mass around m_ϕ from pion-pion annihilation, pn bremsstrahlung, and the direct decay of rho and omega mesons. The most important one is found to come from pion-pion annihilation.

We have considered three scenarios for the kaon and vector meson properties in nuclear medium. The dilepton spectra from phi meson decays, as well as the total dilepton spectra, in the three scenarios show quite different characteristics. We conclude that with a mass resolution of about 1% as to be achieved by the HADES collaboration, it is possible to determine qualitatively whether there are any medium effect on kaon and/or vector mesons. A quantitative determination of the effective masses of kaons and vector mesons from the dilepton spectrum is found to be difficult. However, a combination of the information from the dilepton spectra and other observables such as the phi meson yield from the analysis of K^+K^- channels as well as the kaon yields and spectra will definitely provide good constraints on the in-medium properties of kaons and vector mesons.

Acknowledgement

WSC and CMK were supported in part by the National Science Foundation under Grant No. PHY-9509266 and The Welch Foundation under Grant No. A-1358. GQL was supported in part by the Department of Energy under Contract No. DE-FG02-88Er40388.

[1] J. Pochodzalla, *Prog. Part. Nucl. Phys.* 39 (1997) 443

[2] D. B. Kaplan and A. E. Nelson, *Phys. Lett. B* 175 (1986) 57;
A. E. Nelson and D. B. Kaplan, *Phys. Lett. B* 192 (1987) 193.

[3] C. H. Lee, G. E. Brown, D. P. Min, and M. Rho, *Nucl. Phys. A* 585 (1995) 401.

[4] G. E. Brown and M. Rho, *Phys. Rep.* 269 (1996) 333.

[5] J. W. Harris and B. Müller, *Ann. Rev. Nucl. Part. Sci.* 46 (1996) 71.

[6] G. E. Brown and M. Rho, *Phys. Rev. Lett.* 66 (1991) 2720.

[7] W. Reisdorf and H. G. Ritter, *Ann. Rev. Nucl. Part. Sci.* 48 (1997)

[8] W. Cassing, V. Metag, U. Mosel, and K. Niita, *Phys. Rep.* 188 (1990) 363.

[9] C. M. Ko and G. Q. Li, *J. Phys. G* 22 (1996) 1673.

[10] E. Shuryak, *Phys. Rep.* 67 (1980) 71.

[11] K. Kajantie, J. Kapusta, L. McLerran, and A. Mekjian, *Phys. Rev. D* 34 (1986) 2746.

[12] C. Gale and J. Kapusta, *Phys. Rev. C* 35 (1987) 2107.

[13] G. Q. Li and C. M. Ko, *Nucl. Phys. A* 582 (1995) 731.

[14] G. Roche *et al.* (DLS collaboration), *Phys. Rev. Lett.* 61 (1988) 1069;
C. Naudet *et al.* (DLS collaboration), *Phys. Rev. Lett.* 62 (1989) 2652.

[15] R. J. Porter *et al.* (DLS collaboration), *Phys. Rev. Lett.* 79 (1997) 1229.

[16] W. Koenig, in *Proc. Workshop on Dilepton Production in Relativistic Heavy-Ion Collisions*, ed. H. Bokemeyer (GSI, Darmstadt, 1994).

[17] G. Agakichiev *et al.* (CERES collaboration), *Phys. Rev. Lett.* 75 (1995) 1272;
G. Agakichiev *et al.* (CERES collaboration), *Nucl. Phys. A* 610 (1996) 317c;
A. Drees, *Nucl. Phys. A* 610 (1996) 536c.

[18] M. Masera for the HELIOS-3 collaboration, *Nucl. Phys. A* 590 (1995) 93c;
A.L.S. Angelis *et al.* (HELIOS-3 collaboration), CERN-PPE/97-117.

[19] M. C. Abreu *et al.* (NA38 collaboration), *Phys. Lett. B* 368 (1996) 230;
C. Lourenco, *Nucl. Phys. A* 610 (1996) 552c.

[20] G. Q. Li, C. M. Ko, and G. E. Brown, *Phys. Rev. Lett.* 75 (1995) 4007;
G. Q. Li, C. M. Ko, and G. E. Brown, *Nucl. Phys. A* 606 (1996) 568;
G. Q. Li, C. M. Ko, G. E. Brown, and H. Sorge, *Nucl. Phys. A* 611 (1996) 539.

[21] W. Cassing, W. Ehehalt, and C. M. Ko, *Phys. Lett. B* 363 (1995) 35.

[22] R. Rapp, G. Chanfray, and J. Wambach, *Nucl. Phys. A* 617 (1997) 472.

[23] L. Xiong, Z. G. Wu, C. M. Ko, and J. Q. Wu, *Nucl. Phys. A* 512 (1990) 772.

[24] Gy. Wolf, G. Batko, W. Cassing, U. Mosel, K. Niita, and M. Schäfer, *Nucl. Phys. A* 517 (1990) 615;
Gy. Wolf, W. Cassing, and U. Mosel, *Nucl. Phys. A* 552 (1993) 549.

[25] R. Holzmann *et al.* (TAPS collaboration), *Phys. Rev. C* 56 (1997) R2920.

[26] S. Okubo, *Phys. Lett.* 5 (1963) 165;
J. Iizuka, *Prog. Theo. Phys. Suppl.* 37-38 (1966) 21.

[27] A. Shor, *Phys. Rev. Lett.*, 54 (1985) 1122.

[28] D. Lissauer and E. Shuryak, *Phys. Lett. B* 253 (1991) 15;
E. Shuryak and V. Thorsson, *Nucl. Phys. A* 536 (1992) 739.

[29] T. Hatsuda and S. H. Lee, *Phys. Rev. C* 46 (1992) R34;
T. Hatsuda, *Nucl. Phys. A* 544 (1992) 27c.

[30] R. Ferreira for the NA38 collaboration, *Nucl. Phys. A* 544 (1992) 497c.

[31] M. A. Mazzoni for the HELIOS-3 collaboration, *Nucl. Phys. A* 566 (1994) 95c.

[32] C. M. Ko and B. H. Sa, *Phys. Lett. B* 258 (1991) 6.

[33] M. Berenguer, H. Sorge, and W. Greiner, *Phys. Lett. B* 332 (1994) 15.

[34] P. Koch, U. Heinz, and J. Pisút, *Phys. Lett. B* 243 (1990) 149.

[35] B. A. Cole for the E802 Collaboration, *Nucl. Phys. A* 590 (1995) 179c;
Y. Akiba *et al.* (E802 collaboration), *Phys. Rev. Lett.* 76 (1996) 2021.

[36] P. Braun-Munzinger, J. Stachel, J. P. Wessels, and N. Xu, *Phys. Lett. B* 344 (1995) 43.

[37] J. Cleymans, D. Elliott, H. Satz, and R.L. Thews, *nucl-th/9603004*.

[38] A. J. Baltz and C. Dover, *Phys. Rev. C* 53 (1996) 362.

[39] N. Herrmann for FOPI Collaboration, *Nucl. Phys. A* 610 (1996) 49c.

[40] W. S. Chung, G. Q. Li, and C. M. Ko, *Phys. Lett. B* 401 (1997) 1;
W. S. Chung, G. Q. Li, and C. M. Ko, *Nucl. Phys. A* 625 (1997) 347.

[41] C. M. Ko, V. Koch, and G. Q. Li, *Ann. Rev. Nucl. Part. Sci.* 47 (1997) 505.

[42] X. Jin and D. B. Leinweber, *Phys. Rev. C* 52 (1995) 3344.

[43] M. Asakawa and C. M. Ko, *Nucl. Phys. A* 560 (1993) 399.

[44] F. Klingl, N. Kaiser, and W. Weise, *Nucl. Phys. A* 624 (1997) 527.

[45] S. Leupold, W. Peters, and U. Mosel, *Nucl. Phys. A* 628 (1998) 311.

[46] K. Saito, K. Tsushima, and A. W. Thomas, *Phys. Rev. C* 55 (1997) 2637.

[47] H. C. Jean, J. Pickarewicz, and A. G. Williams, *Phys. Rev. C* 49 (1994) 1981.

[48] H. Shiomo and T. Hatsuda, *Phys. Lett. B* 334 (1994) 281.

[49] C. S. Song, P. W. Xia, and C. M. Ko, *Phys. Rev. C* 52 (1995) 408.

[50] S. A. Chin, *Ann. Phys.* 108 (1977) 301.

[51] M. Herrmann, B. L. Friman, and W. Nörenberg, *Nucl. Phys. A* 560 (1993) 411.

[52] H. Kuwaraba and T. Hatsuda, *Prog. Theor. Phys.* 94 (1995) 1163c.

[53] C. M. Ko, P. Lévai, X. J. Qiu, and C. T. Li, *Phys. Rev. C* 45 (1992) 1400.

[54] F. Klinger, T. Wass, and W. Weiss, *Phys. Lett. B*, in press (hep-ph/9709210).

[55] G. E. Brown, K. Kubodera, and M. Rho, *Phys. Lett. B* 192 (1987) 272.

[56] H. D. Politzer and M. B. Wise, *Phys. Lett. B* 273 (1991) 156.

[57] G. E. Brown, C. H. Lee, M. Rho, and V. Thorsson, *Nucl. Phys. A* 567 (1994) 937.

[58] N. Kaiser, P. B. Siegel, and W. Weise, *Nucl. Phys. A* 594 (1995) 325.

[59] C. H. Lee, *Phys. Rep.* 275 (1996) 255.

[60] T. Waas and W. Weise, *Nucl. Phys. A* 625 (1997) 287.

[61] M. Lutz, A. Steiner, and W. Weise, *Nucl. Phys. A* 574 (1994) 755.

[62] J. Schaffner, A. Gal, I. N. Mishustin, H. Stöcker, and W. Greiner, *Phys. Lett. B* 334 (1994) 268.

[63] R. Knorren, M. Prakash, and P. J. Ellis, *Phys. Rev. C* 52 (1995) 3470.

[64] J. L. Ritman *et al.* (FOPI collaboration), *Z. Phys. A* 352 (1995) 355;
D. Best *et al.* (FOPI collaboration), *Nucl. Phys. A* 625 (1997) 307;
D. Miskowiec *et al.* (KaoS collaboration), *Phys. Rev. Lett.* 72 (1994) 3650;
R. Elmer *et al.* (KaoS collaboration), *Phys. Rev. Lett.* 77 (1996) 4886;
P. Senger for the KaoS collaboration, *Heavy Ion Physics* 4 (1996) 317;
R. Barth *et al.* (KaoS collaboration), *Phys. Rev. Lett.* 78 (1997) 4027.

[65] X. S. Fang, C. M. Ko, G. Q. Li, and Y. M. Zheng, *Nucl. Phys. A* 575 (1994) 766;
G. Q. Li, C. M. Ko, and X. S. Fang, *Phys. Lett. B* 329 (1994) 149;
G. Q. Li, C. M. Ko, and B. A. Li, *Phys. Rev. Lett.* 74 (1995) 235;
G. Q. Li and C. M. Ko, *Nucl. Phys. A* 594 (1995) 460.

[66] G. Q. Li, C. H. Lee, and G. E. Brown, *Phys. Rev. Lett.* 79 (1997) 5214;
G. Q. Li, C. H. Lee, and G. E. Brown, *Nucl. Phys. A* 625 (1997) 372.

[67] W. Cassing, E. L. Bratkovskaya, U. Mosel, S. Teis, and A. Sibirtsev, *Nucl. Phys. A* 614 (1997) 415;
E. L. Bratkovskaya, W. Cassing, and U. Mosel, *Nucl. Phys. A* 622 (1997) 593.

[68] Z. S. Wang, A. Faessler, C. Fuchs, V. S. Uma Maheswari, and D. S. Kosov, *Phys. Rev. Lett.* 79 (1997) 4096;
Z. S. Wang, A. Faessler, C. Fuchs, V. S. Uma Maheswari, and D. S. Kosov, *Nucl. Phys. A*, in press.

[69] G. Q. Li, C. M. Ko, and G. E. Brown, *Phys. Lett. B* 381 (1996) 17.

[70] G. Q. Li and C. M. Ko, *Phys. Rev. C* 54 (1996) R2159.

[71] R. Machleidt, *Adv. Nucl. Phys.* 19 (1989) 189.

[72] A. Baldini *et al.*, *Total cross sections of high energy particles*, (Springer-Verlag, Heidelberg, 1988).

[73] J. Cugnon, P. Deneye, and J. Vandermeulen, *Phys. Rev. C* 41 (1990) 1339.

[74] A. Sibirtsev, *Nucl. Phys. A* 604 (1996) 455.

[75] A. Sibirtsev, W. Cassing, and U. Mosel, *Z. Phys. A* 358 (1997) 357.

[76] Ye. S. Golubeva, L. A. Kondratyuk, and W. Cassing, *Nucl. Phys. A* 625 (1996) 832;
Th. Weidmann, E. L. Bratkovskaya, W. Cassing, and U. Mosel, *nucl-th/9711004*.

[77] A. Sibirtsev and W. Cassing, *nucl-th/9712009*.

[78] K. Tsushima, S. W. Huang, and A. Faessler, *Phys. Lett. B* 337 (1994) 245;
K. Tsushima, S. W. Huang, and A. Faessler, *J. Phys. G* 21 (1995) 33.

[79] G. Q. Li and C. M. Ko, *Nucl. Phys. A* 594 (1995) 439;
G. Q. Li, C. M. Ko, and W. S. Chung, *Phys. Rev. C* 57 (1998).

[80] A. Sibirtsev, W. Cassing, and C. M. Ko, *Z. Phys. A* 358 (1997) 101.

[81] C. M. Ko, *Phys. Lett. B* 120 (1983) 294; *B* 138 (1984) 361.

[82] H. Joos, *Phys. Lett. B* 24 (1967) 103.

[83] C. M. Ko, Q. Li, and R. Wang, *Phys. Rev. Lett.* 59 (1987) 1084;
C. M. Ko and Q. Li, *Phys. Rev. C* 37 (1988) 2270;
Q. Li, J. Q. Wu, and C. M. Ko, *Phys. Rev. C* 39 (1989) 849.